Available online at www.sciencedirect.com
ScienceDirect
Journal of Magnetic Resonance 191 (2008) 315–321
JMR Journal of Magnetic Resonance
www.elsevier.com/locate/jmr

Nuclear relaxation effects in Davies ENDOR variants

John J.L. Morton [a,b,*], Nicholas S. Lees [c], Brian M. Hoffman [c], Stefan Stoll [d]

[a] Department of Materials, Oxford University, Oxford OX1 3PH, UK
[b] Clarendon Laboratory, Department of Physics, Oxford University, Oxford OX1 3PU, UK
[c] Department of Chemistry, Northwestern University, Evanston, IL 60208-3003, USA
[d] Department of Chemistry, University of California, Davis, CA 95616, USA

Received 22 August 2007; revised 5 November 2007
Available online 16 January 2008

Abstract

A recent article by Yang and Hoffman [T.-C. Yang, B.M. Hoffman, J. Magn. Reson., 181 (2006) 280] presents a 'Davies/Hahn ENDOR multi-sequence' in which the α and β peaks of an electron-nuclear double resonance (ENDOR) spectrum can be distinguished. This represents one instance of a family of ENDOR sequences which have no initial microwave inversion pulse, and which can reveal information about nuclear relaxation rates and the signs of hyperfine coupling constants. Here we discuss the more general set of such sequences, which we refer to as *Saturated Pulsed ENDOR*, and show how signal sensitivity can be optimised within the context of this new technique. Through simulations, we compare its performance to other techniques based on Davies ENDOR, and experimentally illustrate its properties using the non-heme Fe enzyme anthranilate dioxygenase AntDO. Finally, we suggest a protocol for extracting both the magnitude and sign of the hyperfine tensor using a combination of ENDOR techniques.

Keywords: ENDOR; Nuclear relaxation; Anthranilate dioxygenase; Hyperfine tensor

1. Introduction

Electron-nuclear double resonance (ENDOR) represents a family of techniques in which a combination of radiofrequency (rf) and microwave (mw) excitation is used to study nuclear spins which are coupled to a paramagnetic species [1,2]. A recent paper by Yang and Hoffman [3] discusses the effects of rapidly repeating an ENDOR sequence at a rate commensurate with the relevant spin relaxation times, building on the work of Epel et al. [4]. It is shown how a steady-state ENDOR signal is obtained by repeating a sequence which is similar to the Davies ENDOR method but without the preparatory π mw pulse.

A typical ENDOR spectrum representing a nucleus with spin $I = 1/2$ coupled to an electron spin $S = 1/2$ consists of a pair of peaks with equal intensity at frequencies ν_α and ν_β, associated with the $m_S = +1/2$ (α) and $m_S = -1/2$ (β) electron spin projections. The main advantage of the approach of Yang and Hoffman is the distinguishability of these α and β ENDOR peaks, as their method yields intensities of different magnitude or of different sign. A prerequisite for asymmetry is that the temperature, T, must be around or below the Zeeman temperature $h\nu_{mw}/k_B$ (e.g. 1.7 K for a spectrometer frequency of $\nu_{mw} = 35$ GHz), along with the condition of a suitable combination of relaxation rates of the electron and nuclear spin. The observation of asymmetry in peak intensity permits the determination of the sign of the hyperfine coupling constant and the simplification of a potentially busy spectrum. Furthermore, the intensity difference of the two peaks diminishes as the repetition time is increased, providing a way to measure nuclear spin relaxation processes.

Under similar, but less general, circumstances, the standard Davies ENDOR experiment also yields peaks of unequal intensity, giving access to the sign of the hyperfine coupling constant and to nuclear spin relaxation times [5].

* Corresponding author. Address: Clarendon Laboratory, Department of Physics, Oxford University, Oxford OX1 3PU, UK.
E-mail address: john.morton@sjc.ox.ac.uk (J.J.L. Morton).

1090-7807/$ - see front matter © 2008 Elsevier Inc. All rights reserved.
doi:10.1016/j.jmr.2008.01.006

An alternative method for measuring nuclear spin relaxation via another modified Davies ENDOR sequence is described in [6].

In this work, we compare the method proposed by Yang and Hoffman to other Davies ENDOR variants with respect to their ability to yield asymmetric spectra. The first section summarises the underlying theory. In the following sections, simulations are discussed and an experimental comparison is given. Finally, we draw conclusions about the benefits of the various techniques.

2. Theory

The standard Davies ENDOR sequence is shown in Fig. 1A. It consists of a selective mw and a selective rf π pulse followed by a non-selective two-pulse echo sequence. In the sequence in Fig. 1B, an additional selective rf π pulse is added *after* the echo detection ([6]). This essentially undoes the nuclear spin polarisation created by the first rf pulse and increases the overall intensity of the ENDOR spectrum compared to the standard sequence, thus allowing higher repetition rates. We shall denote this the *Tidy* Davies sequence. In the sequence in Fig. 1C, the initial preparation π pulse is removed, and instead the sequence is repeated sufficiently rapidly so as to drive the electron spin into saturation. This sequence is a generalisation of the one used by Yang and Hoffman (where $t_{mix} \approx 0$) ([3]). As they first noted, the mw π pulse is not necessary to observe an ENDOR effect, since the subsequent two-pulse sequence can act both as an electron polarisation detector and generator. We shall denote this the *Saturated Pulsed* ENDOR sequence, or SP-ENDOR. In contrast to the standard and *Tidy* sequences, the mw $\pi/2$ pulse in SP-ENDOR must be a selective pulse, as it assumes in addition the function of the selective π pulse used in the other variants. This distinction is, of course, unimportant when a single microwave channel is employed, as the preparation π-pulse of a Davies ENDOR sequence must be selective.

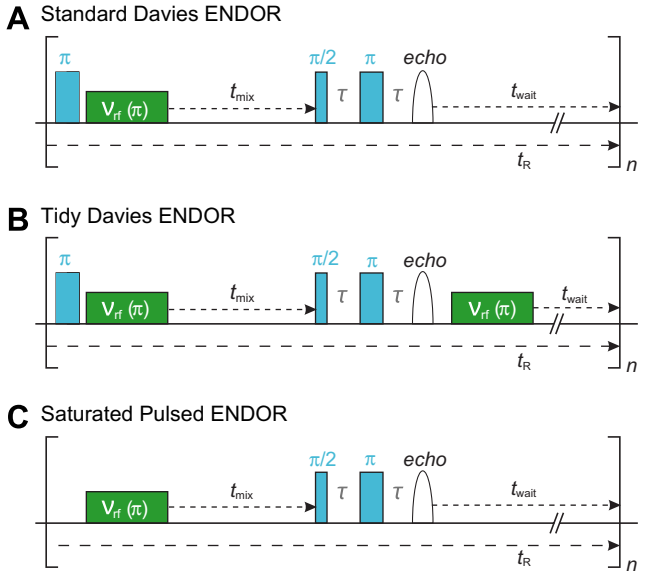

Fig. 1. Davies ENDOR sequence and modifications. (A) Standard Davies sequence, (B) *Tidy* Davies ENDOR: rf π pulse applied after the echo, (C) *Saturated Pulsed* ENDOR sequence: initial mw π pulse omitted. n is the number of repetitions of the sequence in brackets before the radiofrequency is changed.

For all sequences, the mixing time t_{mix} denotes the free-evolution time *before* the two-pulse echo sequence, and the wait time t_{wait} indicates the free-evolution time *after* the two-pulse sequence. The sequence in square brackets is repeated n times. All other inter-pulse delays and all pulses are assumed to be of negligible duration compared to t_{mix} and t_{wait}. The repetition time $t_R \approx t_{mix} + t_{wait}$ is the elapsed time between the first pulse in one sequence and the first pulse in the subsequent one.

An ENDOR spectrum of an $I = 1/2$ nucleus coupled to an $S = 1/2$ electron spin consists of two lines with frequencies ν_α and ν_β and intensities I_α and I_β. For an isotropic hyperfine coupling a_{iso}, the frequencies are

$$\nu_\alpha = |\, \nu_I + a_{iso}/2 \,|, \quad \nu_\beta = |\, \nu_I - a_{iso}/2 \,|, \tag{1}$$

where $\nu_I (= -g_n \beta_n B_0/h)$ is the nuclear Larmor frequency. The intensities are determined by several factors. The nuclear transition matrix elements for the two lines are identical, and the factor mainly responsible for asymmetry is the difference in polarisations of the two nuclear transitions. Effects like the hyperfine enhancement and experimental imperfections of the rf excitation can also render the two intensities unequal. However, these effects are often negligible in high-field ENDOR.

To best describe the intensity features of an ENDOR experiment for our purpose, we introduce two parameters. The first describes the intensity of the strongest peak in the spectrum

$$I = \max\left(|\, I_\alpha \,|, |\, I_\beta \,|\right). \tag{2}$$

The second one quantifies the asymmetry of the ENDOR spectrum

$$A = \frac{I_\alpha - I_\beta}{2I}. \tag{3}$$

For symmetric spectra, the asymmetry parameter gives $A = 0$. $A > 0$ means that the α peak is stronger, whereas $A < 0$ indicates a stronger β peak. The greatest asymmetry is represented by $A = \pm 1$.

I_α and I_β depend on the initial equilibrium polarisation, which in turn is a function of the temperature T and the spectrometer frequency ν_{mw}. In addition, I_α and I_β depend on t_{wait} and t_{mix} as well as on the electron and nuclear spin–lattice relaxation rates T_{1e}^{-1} and T_{1n}^{-1} and the electron-nuclear cross relaxation rate T_{1x}^{-1}. In paramagnetic systems, nuclei usually relax via coupling to the local electron spin, or else to neighbouring electron spins ([5,7]). The direct nuclear spin–lattice relaxation rate can thus be neglected, so that we can assume $T_{1n}^{-1} \approx 0$.

In an ENDOR experiment where the objective is to measure principal values and tilt angles of hyperfine and quadrupole tensors, I should be maximised and A minimised. In

contrast, if α/β peak assignment is of interest, a significant asymmetry A must be achieved without excessive reduction in the overall intensity I. The dependence of the asymmetry on t_{mix} or t_{wait} can also be used to provide insight into relaxation processes. In all cases, the repetition time t_R ($\approx t_{mix} + t_{wait}$) should be as short as possible to maximise signal/time.

3. Simulations

The variation of the overall intensity I and the asymmetry A for the various sequences as a function of t_{mix} and t_{wait} depends on how fast the nuclei relax compared to the electrons and compared to the time scale of t_{mix} and t_{wait}. Three physical regimes can be distinguished: (i) $T_{1x} \gg T_{1e}$, (ii) $T_{1x} \approx T_{1e}$ and (iii) $T_{1x} \ll T_{1e}$. The last one is seldom encountered (requiring high electron spin concentrations) and furthermore, T_{1x} and T_{1e} are difficult to distinguish in inversion and saturation recovery experiments. However, by using the ENDOR sequences described here with different delay times, it may be possible to separate the two.

Analytical expressions for the steady-state signals obtained by these ENDOR sequences are rather lengthy, so numerical simulations are better suited to illustrate their dependence on the delay times t_{mix} and t_{wait}. Sample simulations are shown in Figs. 2 and 3. For simplicity, we plot the cases where one of t_{mix} or t_{wait} is set to zero while the other is varied, each corresponding to a potential one-dimensional relaxation experiment [4,5]. The procedure used in simulating the signals is based on Ref. [4], and the details are summarised in Appendix A.

As a general observation, the simulated intensities and asymmetries are multiexponentials with decay constants on the order of T_{1x}^{-1} and T_{1e}^{-1} both along t_{mix} and t_{wait}. The initial rise in intensity from zero is on the scale of $T_{1e}^{-1} + T_{1x}^{-1}$. Analytical expressions of the relevant decay constants are given at the end of Appendix A.

Tidy Davies ENDOR gives the strongest overall ENDOR intensity in experiments where $t_{mix} = 0$ and t_{wait} is varied (see Fig. 2A), for all T_{1x}/T_{1e} regimes. On the other hand, SP-ENDOR yields the greatest intensities in experiments with $t_{wait} = 0$ and t_{mix} variable (see Fig. 2B). It is apparent from Fig. 2 that, for a given repetition time, standard and Tidy Davies ENDOR are best performed with $t_{mix} = 0$, as their intensities for $t_{wait} = 0$ are very small.

The obtainable asymmetry depends strongly on the sequence and on the ratio T_{1x}/T_{1e}. Except for standard Davies with $t_{mix} = 0$, the asymmetry is always negative, i.e. the β peak intensity is less negative/more positive than the α peak intensity. For all T_{1x}/T_{1e}, spectra acquired with the Tidy sequence are essentially symmetric for $t_{mix} = 0$, but their asymmetry for $t_{wait} = 0$ and long t_{mix} is unexpectedly similar to the ones obtained by the other sequences. The asymmetry of spectra from the standard Davies and SP-ENDOR sequences is very sensitive to the T_{1x}/T_{1e} ratio: the slower the cross relaxation, the stronger the asymmetry. SP-ENDOR asymmetry does not vary much as a function of t_{wait} if $t_{mix} = 0$, whereas the asymmetry decreases for increasing t_{wait} in standard Davies. With $t_{wait} = 0$, standard Davies and SP-ENDOR are similar in asymmetry.

Yang and Hoffman originally proposed to use the SP-ENDOR sequence with $t_{mix} = 0$ and a substantial t_{wait} in

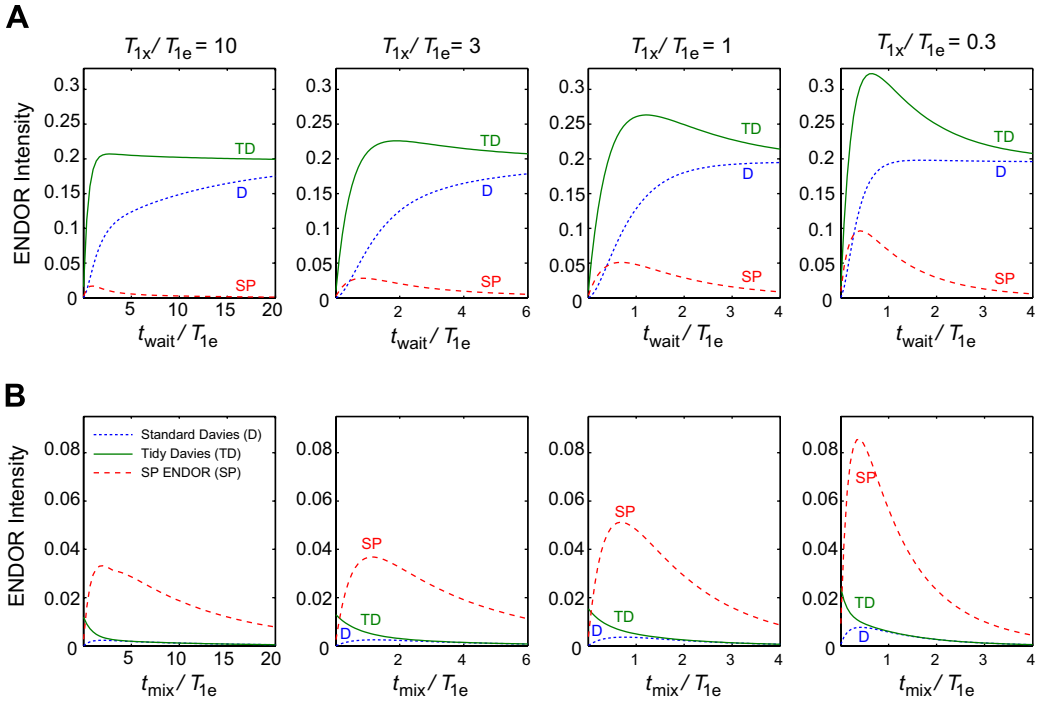

Fig. 2. Dependence of ENDOR intensity (see Eq. (2)) on t_{mix} and t_{wait} for the Davies ENDOR sequence and its modifications, given different ratios of T_{1x} and T_{1e}. (A) $t_{mix} = 0$ and t_{wait} is varied; (B) $t_{wait} = 0$ and t_{mix} is varied. Simulation parameters: $\nu_{mw} = 35$ GHz, $T = 2$ K, $T_{1n} = \infty$, $A > 0$.

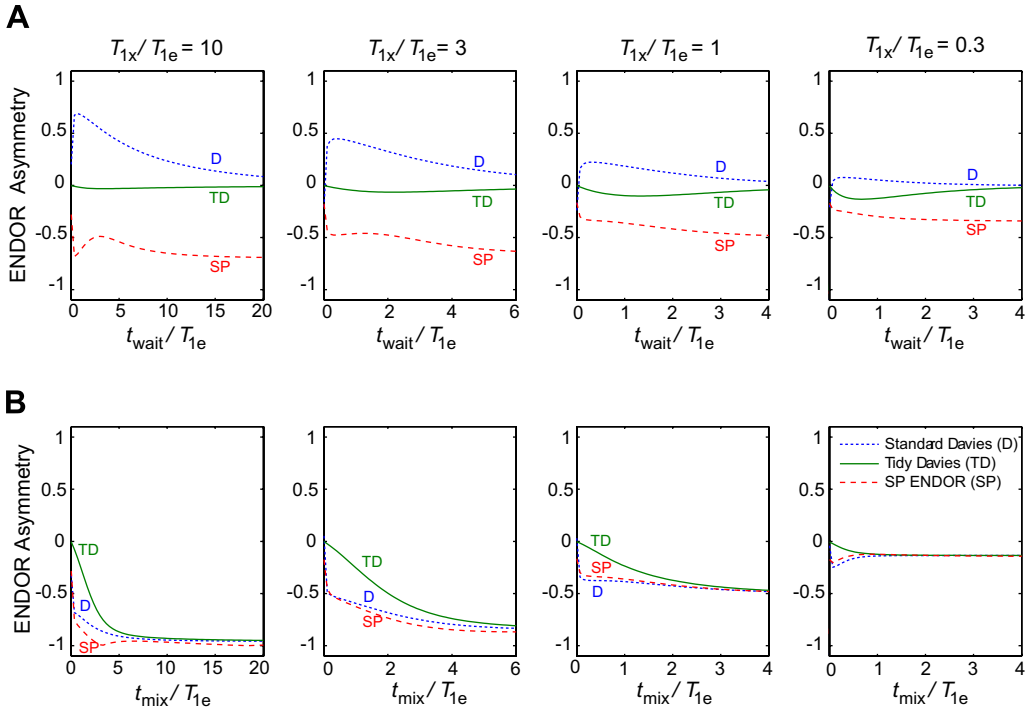

Fig. 3. Dependence of ENDOR asymmetry (see Eq. (3)) on t_{mix} and t_{wait} for the Davies ENDOR sequence and its modifications, given different ratios of T_{1x} and T_{1e}. (A) $t_{mix} = 0$ and t_{wait} is varied; (B) $t_{wait} = 0$ and t_{mix} is varied. Simulation parameters: $\nu_{mw} = 35$ GHz, $T = 2$ K, $T_{1n} = \infty$, $A > 0$.

order to measure asymmetry (this so-called Davies/Hahn multi-sequence comprises an rf pulse prior to the Hahn detection sequence). However, it is apparent by comparing Fig. 2A and B that when $T_{1x} \gg T_{1e}$, slightly greater intensity and significantly greater asymmetry is obtained if t_{wait} is set to zero and t_{mix} is substantial. The resulting sequence resembles the reverse of the Davies/Hahn multi-sequence proposed, i.e. the rf pulse immediately *follows* the electron spin echo detection instead of preceding it. Under these conditions (small t_{wait}, finite t_{mix}), the SP-ENDOR signal intensity can substantially exceed that of the standard and Tidy sequences. When $T_{1x} = T_{1e}$, the SP-ENDOR signal is symmetric with respect to t_{mix} and t_{wait}, i.e. neither the intensity nor the asymmetry change if the values of t_{mix} and t_{wait} are exchanged. In this regime, it does not matter whether the rf pulse precedes or follows the two-pulse echo sequence.

With decreasing T_{1x}/T_{1e} it becomes increasingly difficult to generate substantial asymmetry, although the overall intensity increases for all three sequences. For $t_{mix} \approx 0$, the standard and Tidy sequences give primarily symmetric spectra with good intensity. SP-ENDOR produces the greatest observable asymmetry, but at the cost of reduced overall intensity. All three sequences give only small asymmetry for $t_{wait} \approx 0$ and $t_{mix} > 0$.

The simulations above assume ideal pulses (precise rotational angles, perfect selectivity where required, etc.), while real experiments on inhomogeneously broadened lines with pulses of finite length fall substantially short of such perfection. As one lowers the selectivity of the relevant pulses in each ENDOR variant (initial inversion pulse for standard and Tidy Davies, $\pi/2$ pulse in SP-ENDOR) the ENDOR intensity falls accordingly, though SP-ENDOR shows a marginally lower sensitivity to a loss of selectivity, compared with the standard and Tidy sequences.

4. Experiment

In this section, we use the non-heme Fe enzyme anthranilate dioxygenase, AntDO [8,9] to illustrate the properties of the SP-ENDOR sequence described in the simulations above. Previous ENDOR studies on this enzyme indicate that $T_{1x} > T_{1e}$ at 2 K, making it an appropriate spin system for studies of asymmetry in ENDOR spectra ([3]). Experiments were performed using a lab-built Q-band ENDOR spectrometer described in Ref. [10], with a sample concentration of 1 mM. The experimental ENDOR intensity is defined in absolute terms (as opposed to a percentage of the echo intensity), and the asymmetry as in Eq. (3).

We begin by comparing ^{14}N signals from SP-ENDOR sequences with (long t_{mix}, short t_{wait}) versus (short t_{mix}, long t_{wait}), as shown in Fig. 4A. The fact that (long t_{mix}, short t_{wait}) yields both a greater intensity and a greater asymmetry is an immediate confirmation that $T_{1x} > T_{1e}$ in this system. Fig. 4B shows simulated α and β peak intensities for the two pulse sequences used. Comparison of these plots with the data shown above indicates that T_{1x} is approximately in the range $2T_{1e} < T_{1x} < 10T_{1e}$. Furthermore, the fact that the α peak is of smaller intensity than the β peak (negative asymmetry) indicates that the hyperfine constant here is positive, by comparison with Fig. 3B. Fig. 4A also shows an asymmetry in the ^{1}H ENDOR signals, and an enhancement in intensity when long t_{mix} with short t_{wait} is used.

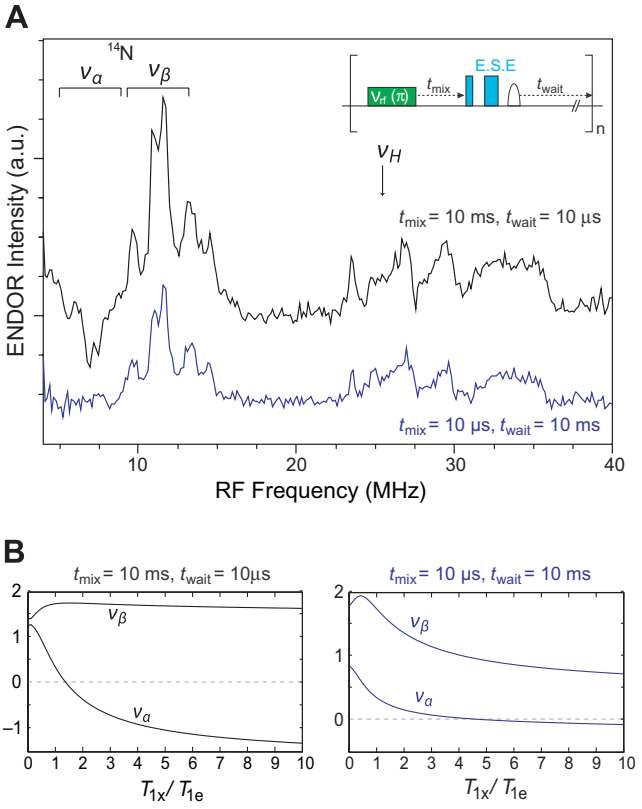

Fig. 4. (A) Q-band ENDOR spectra for natural abundance AntDO collected using the SP-ENDOR sequence with (bottom) $t_{mix} = 10$ µs, $t_{wait} = 10$ ms and (top) $t_{mix} = 10$ ms, $t_{wait} = 10$ µs. Both the intensity and asymmetry of the spectrum are enhanced by shortening t_{wait} and lengthening t_{mix}. Experimental parameters: enzyme concentration 1 mM, $\nu_{mw} = 34.771$ GHz, B_0 field = 602.1 mT, $T = 2$ K, mw $\pi/2$ pulse length 40 ns, $\tau = 700$ ns, rf π pulse length 10 µs. (B) Simulated peak intensities for the two pulse sequences shown in (A). Simulation parameters: $\nu_{mw} = 34.8$ GHz, $T = 2$ K, $T_{1e} = 6$ ms.

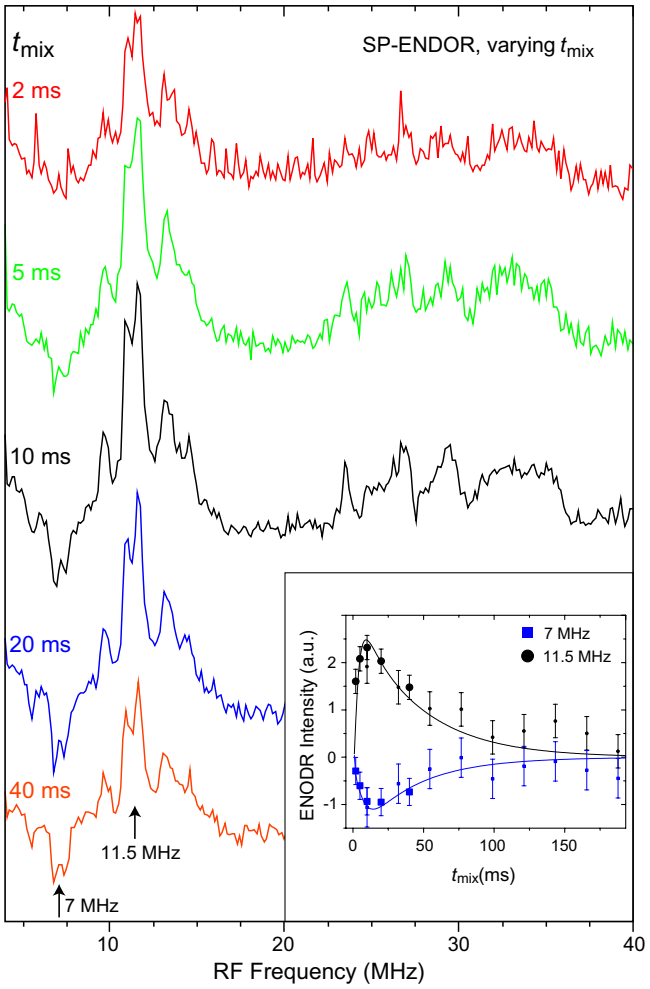

Fig. 5. Q-band ENDOR spectra for natural abundance AntDO collected using the SP-ENDOR sequence with $t_{wait} = 10$ µs, and at a range of different t_{mix}. The inset shows integrated peak intensities for the α and β peaks (at 11.5 and 7.0 MHz, respectively). Large symbols are obtained by integrating the five traces shown above in the range 6.54 to 8.09 MHz and 10.64 to 12.61 MHz and subtracting a baseline. Smaller symbols are plotted on an independent y-axis, and were obtained by sitting at a particular rf frequency and varying shot repetition time and subtracting results obtained with an off-resonance rf pulse. Peak intensities were fit to the model described in the text, using $T_{1e} = 6.4$ ms and yielding $T_{1x} \approx 50$ ms (solid lines). Experimental parameters as in Fig. 4.

Having minimised t_{wait}, we now vary t_{mix} to trace out the behaviour predicted by the simulation in Fig. 2B. The resulting spectra are shown in Fig. 5, with the inset comparing the trend of ENDOR intensity with our model. T_{1e} was measured separately via an inversion recovery sequence, yielding a good mono-exponential fit with a time constant of $T_{1e} = 6.4$ ms. This value was incorporated into the model used to fit to the data, yielding $T_{1x} = 50$ ms. Both the positive and negative α and β peak intensities were fit to the same time parameter (T_{1x}).

While the above data provide a convenient illustration of the relaxation effects described in this work for the case $T_{1x} \approx 8T_{1e}$, a study of other species (with different ratios of T_{1x} and T_{1e}), and a thorough two-dimensional experiment where both t_{mix} and t_{wait} are swept are required to test the simulations in all conditions. This is the subject of a future work.

5. Conclusions

There is no single ENDOR sequence that is optimal under all experimental circumstances, and the choice of technique depends on precisely what information is being sought.

If the principal values of the hyperfine and quadrupole tensors are of interest, a maximal ENDOR intensity with minimal asymmetry is desired, and in this case the Tidy Davies sequence ([6]) is most effective, especially for slow and medium cross relaxation. However, for low-temperature work, one should be conscious of the possibility of sample heating from a second rf pulse, and assess the advantage of Tidy Davies over the standard sequence accordingly.

To extract signs of the hyperfine interaction it is necessary to introduce an asymmetry between the α and β ENDOR peak intensities. In general, asymmetry can only be obtained at the cost of signal intensity. However, use

of either SP-ENDOR or standard Davies ENDOR maximises the asymmetric signal which can be acquired in the shortest time, when the rf pulse immediately follows the two-pulse echo detection ($t_{\rm wait} \ll t_{\rm mix}$). A protocol for the complete measurement of the hyperfine tensor would therefore be:

(I) Tidy Davies ENDOR, for optimum ENDOR intensity to extract principal values. $t_{\rm mix}$ can be short, but $t_{\rm wait}$ should be 2–4 times $T_{1\rm e}$, depending on nuclear relaxation times (shorter for shorter $T_{1\rm x}$).
(II) SP-ENDOR for maximum ENDOR asymmetry to extract signs. $t_{\rm wait}$ should be kept short (a few microseconds), while $t_{\rm mix}$ should be approximately $T_{1\rm e}$.

Acknowledgments

J.J.L.M. is supported by St. John's College, Oxford. S.S. acknowledges the support of the Swiss National Science Foundation. B.M.H. acknowledges support of the US NIH HL13531.

Appendix A. The model

The model [4] used for computing the ENDOR intensities neglects all coherences generated by the pulses and uses the populations n_i of the four states i of an $S = I = 1/2$ spin system, written as a vector

$$\boldsymbol{n} = (n_1, n_2, n_3, n_4)^{\rm T}. \tag{A.1}$$

The levels are numbered from the lowest to the highest in energy (1 and 2: electron β, 3 and 4: electron α). The initial normalised equilibrium populations are

$$\boldsymbol{n}_{\rm eq} = \frac{(1, 1, \epsilon, \epsilon)^{\rm T}}{2 + 2\epsilon}, \text{ with } \epsilon = \exp\left(-\frac{h\nu_{\rm mw}}{\mu_{\rm B} T}\right). \tag{A.2}$$

For the experimental conditions used in this article ($\nu_{\rm mw} = 34.8$ GHz, $T = 2$ K), $\epsilon = 0.43$.

The selective mw π pulse exchanges populations n_1 and n_3. The two-pulse detection sequence, which is assumed to be non-selective for standard and Tidy Davies ENDOR, equalises n_1 and n_3, and n_2 and n_4. For SP-ENDOR, the two-pulse sequence is chosen selective, equalising n_1 and n_3 while n_2 and n_4 remain unaffected. We note that the ENDOR response is independent of the particular electron spin transition excited, and hence the results would be the same for pulses acting between levels 2 and 4. The selective α (β) rf π pulse exchanges the populations n_3 and n_4 (n_1 and n_2).

All time intervals except $t_{\rm mix}$ and $t_{\rm wait}$ are neglected, as they are usually very short compared to $T_{1\rm e}$ and $T_{1\rm x}$, which determine the intensity and asymmetry of the ENDOR peaks. During the free evolution times $t_{\rm mix}$ and $t_{\rm wait}$, $\boldsymbol{n}$ changes according to

$$\frac{\rm d}{{\rm d}t}\boldsymbol{n}(t) = -\boldsymbol{\Gamma}\boldsymbol{n}(t) \tag{A.3}$$

with the asymmetric relaxation matrix,

$$\boldsymbol{\Gamma} = \begin{pmatrix} \Gamma_{\rm n} + \epsilon\Gamma_{\rm e} + \epsilon\Gamma_{\rm x} & -\Gamma_{\rm n} & -\Gamma_{\rm e} & -\Gamma_{\rm x} \\ -\Gamma_{\rm n} & \Gamma_{\rm n} + \epsilon\Gamma_{\rm e} + \epsilon\Gamma_{\rm x} & -\Gamma_{\rm x} & -\Gamma_{\rm e} \\ -\epsilon\Gamma_{\rm e} & -\epsilon\Gamma_{\rm x} & \Gamma_{\rm n} + \Gamma_{\rm e} + \Gamma_{\rm x} & -\Gamma_{\rm n} \\ -\epsilon\Gamma_{\rm x} & -\epsilon\Gamma_{\rm e} & -\epsilon\Gamma_{\rm n} & \Gamma_{\rm n} + \Gamma_{\rm e} + \Gamma_{\rm x} \end{pmatrix}, \tag{A.4}$$

Here it is assumed that the relaxation times for the two forbidden EPR transitions (1–4 and 2–3) are identical. The electron spin–lattice relaxation time $T_{1\rm e}$, the nuclear spin–lattice relaxation time $T_{1\rm n}$, and the electron-nuclear cross relaxation time $T_{1\rm x}$ are related to the elements in the relaxation matrix by

$$T_{1\rm e}^{-1} = (1+\epsilon)\Gamma_{\rm e}, \quad T_{1\rm n}^{-1} = 2\Gamma_{\rm n}, \quad T_{1\rm x}^{-1} = (1+\epsilon)\Gamma_{\rm x}. \tag{A.5}$$

In paramagnetic systems, $T_{1\rm n}$ is in general much larger than $T_{1\rm x}$ and $T_{1\rm e}$. We thus can set $T_{1\rm n}^{-1} = 0$.

The echo amplitude is obtained by computing $V = n_1 - n_3$ *before* the application of the two-pulse sequence (which equalises n_1 and n_3). The intensities of the α and β ENDOR peaks are then obtained by

$$I_\alpha = V_\alpha - V_{\rm off} \qquad I_\beta = V_\beta - V_{\rm off}, \tag{A.6}$$

where V_α and V_β are the echo amplitudes with the rf pulse resonant on the nuclear transition in the α (β) electron manifold, and $V_{\rm off}$ is the echo amplitude when the rf pulse is off-resonant.

The sequence is computed n times, where in this paper we use $n = 50$. The n echo amplitudes are averaged. However, the difference between this average and the last echo amplitude is small. A steady-state is usually reached already after a couple of repetitions.

In principle, the steady-state populations can be computed analytically, but the resulting expressions are of unmanageable length. However, the characteristic relaxation constants along $t_{\rm mix}$ and $t_{\rm wait}$ given by the eigenvalues of the relaxation matrix in Eq. (A.4) (with $\Gamma_{\rm n} = 0$) can be expressed in a compact form. In terms of the relaxation times as given in Eq. (A.5) they are

$$\begin{aligned} \lambda_1 &= 0 & \lambda_3 &= \tfrac{1}{2}\left[T_{1\rm e}^{-1} + T_{1\rm x}^{-1} + \Delta\lambda\right] \\ \lambda_2 &= T_{1\rm e}^{-1} + T_{1\rm x}^{-1} & \lambda_4 &= \tfrac{1}{2}\left[T_{1\rm e}^{-1} + T_{1\rm x}^{-1} - \Delta\lambda\right] \end{aligned} \tag{A.7}$$

where

$$\Delta\lambda = \sqrt{\left(T_{1\rm e}^{-1} + T_{1\rm x}^{-1}\right)^2 - 16\frac{\epsilon}{(1+\epsilon)^2} T_{1\rm e}^{-1} T_{1\rm x}^{-1}} \tag{A.8}$$

The relaxation rate λ_2 is always the largest. λ_3 decreases from $T_{1\rm e}^{-1} + T_{1\rm x}^{-1}$ to $T_{1\rm e}^{-1}$ as ϵ is increased from 0 (no thermal polarisation) to 1 (complete thermal polarisation). At the same time, λ_4 increases from 0 to $T_{1\rm x}^{-1}$. For our experimental case of $\epsilon = 0.43$ and $T_{1\rm x}/T_{1\rm e} \approx 8$, the three non-zero decay constants are $\lambda_2/T_{1\rm e}^{-1} = 1.125$, $\lambda_3/T_{1\rm e}^{-1} = 1.022$, and $\lambda_4/T_{1\rm e}^{-1} = 0.103$.

References

[1] G. Feher, Phys. Rev. 114 (1959) 1219.
[2] E.R. Davies, Phys. Lett. A 47 (1974) 1.
[3] T.-C. Yang, B.M. Hoffman, J. Magn. Reson. 181 (2006) 280.
[4] B. Epel, A. Poppl, P. Manikandan, S. Vega, D. Goldfarb, J. Magn. Reson. 181 (2001) 148.
[5] S. Stoll, B. Epel, S. Vega, D. Goldfarb, J. Chem. Phys. 127 (2007) 164511.
[6] A.M. Tyryshkin, J.J.L. Morton, A. Ardavan, S.A. Lyon, J. Chem. Phys. 124 (2006) 234508.
[7] A. Abragam, M. Goldman, Principles of dynamic nuclear-polarization, Rep. Prog. Phys. 41 (1978) 395–467.
[8] D.M. Eby, Z.M. Beharry, E.D. Coulter, D.M. Kurtz Jr., E.L. Neidle, J. Bacteriol. 183 (2001) 109.
[9] Z.M. Beharry, D.M. Eby, E.D. Coulter, R. Viswanathan, E.L. Neidle, R.S. Phillips, D.M. Kurtz Jr., Biochemistry 42 (2003) 13625.
[10] C.E. Davoust, P.E. Doan, B.M. Hoffman, J. Magn. Res. A 119 (1996) 38.